Biochimica et Biophysica Acta, 1029 (1990) 33–42
Elsevier

BBAMEM 75029

Non-selective cation channel on pancreatic duct cells

Michael A. Gray and Barry E. Argent

Department of Physiological Sciences, University Medical School, Newcastle upon Tyne (U.K.)

(Received 12 March 1990)

Key words: Patch clamp; Ion channel; Secretion; Pancreatic duct; (Rat)

We have identified a non-selective cation channel on pancreatic duct cells. These epithelial cells secrete the bicarbonate ions found in pancreatic juice; a process controlled by the hormone secretin, which uses cyclic AMP as an intracellular messenger. The non-selective channel is located on both apical and basolateral plasma membranes of the duct cell, is equally permeable to sodium and potassium, and has a linear I/V relationship with a single-channel conductance of about 25 pS. Channel opening requires the presence of 1 μM Ca^{2+} on the cytoplasmic face of the membrane, and is also increased by depolarization. Intracellular ATP, ADP, magnesium, and a rise in pH all decreased channel activity. The channel was not affected by 10 mM TEA, 1 mM Ba^{2+} or 0.5 mM decamethonium applied to the cytoplasmic face of the membrane, but 0.5 mM quinine caused a flickering block which was more pronounced at depolarizing potentials. We observed the channel only rarely in cell-attached patches on unstimulated duct cells, and acute exposure to stimulants did not cause channel activation. However, after prolonged stimulation, the proportion of cell-attached patches containing active channels was increased 9-fold. The role of this channel in pancreatic duct cell function remains to be elucidated.

Introduction

Non-selective cation channels have been identified in the plasma membranes of many different cells (for a review see Ref. 1). Typically, these channels are equally permeable to sodium and potassium but impermeant to anions, have single-channel conductances in the range 20–35 pS, and are activated by calcium ions. Where it has been measured, the divalent cation permeability is usually very low [2,3]; however, a non-selective cation channel which is equally permeable to sodium and calcium has been described on human neutrophils [4].

Although this class of ion channel is widely distributed, establishing its physiological role has proved difficult in all but a few cell types. In rat and mouse pancreatic acini, non-selective cation channels are activated following stimulation by agonists which increase intracellular calcium, and are thought to be important in maintaining fluid secretion by providing a cellular route for sodium, and possibly calcium, uptake into the cell [5–7]. The same may apply in rat lacrimal cells [8]. although in these cells a strong, sustained, stimulation is necessary to activate the channels [8]. More recently, a non-selective cation channel in renal collecting ducts has been shown to be inhibited by atrial natriuretic peptide (ANP), probably by a direct effect of cyclic GMP which is increased in ANP-treated cells [9,10]. The same channel is also inhibited by amiloride, and so could represent the amiloride-sensitive conductive pathway which mediates electrogenic sodium absorption [9,10]. In excitable tissue, non-selective cation channels may contribute to pacemaker potentials by providing a maintained depolarizing current, as demonstrated in *Helix* burster neurons [11].

Here we describe the properties of a non-selective cation channel on pancreatic duct cells. These epithelial cells secrete the bicarbonate ions found in pancreatic juice; a process controlled by the hormone secretin, which uses cyclic AMP as an intracellular messenger [12]. We find that non-selective cation channels are located on both apical and basolateral membranes of the duct cell, are regulated by voltage, calcium, magnesium, pH and adenine nucleotides, and are activated after prolonged stimulation. A preliminary report on some of our results has already been published [13].

Methods and Materials

Isolation of pancreatic ducts and ductal epithelial cells

Small interlobular pancreatic ducts were isolated from the glands of copper-deficient rats as previously de-

Correspondence: M.A. Gray, Department of Physiological Sciences, University Medical School, Framlington Place, Newcastle upon Tyne, NE2 4HH, U.K.

scribed [14], and maintained in culture for up to 3 days [15]. Copper-deficiency causes a non-inflammatory atrophy of enzyme-secreting acinar cells, but leaves the duct cells structurally and functionally intact. We have previously shown that these isolated ducts possess morphological, biochemical and secretory characteristics typical of ducts within the intact copper-replete rat pancreas [14,15]. Epithelial cells were isolated from cultured ducts using a combination of enzyme dissociation (papain 4.5 U/ml; Sigma, Poole, U.K.) followed by mechanical disruption in a calcium and magnesium-free solution containing 2 mM EGTA [16].

Electrophysiology

Most experiments were performed on epithelial cells within cultured ducts. The basolateral membrane was exposed by microdissecting away the surrounding connective tissue, while access to the apical membrane was gained by tearing a flap in the wall of the duct. Once studies on the intact ducts had established that the cation channel was present on both apical and basolateral membranes, some experiments were also performed on isolated duct cells.

An intact duct, or a microwell containing single epithelial cells, was placed in a tissue bath mounted on a Nikon Diaphot inverted microscope (Nikon, U.K.), and the cells viewed using phase contrast optics. The bath volume was 2.0 ml, and solution changes were accomplished by gravity feed from reservoirs at a flow rate of 5 $ml \cdot min^{-1}$. Single-channel current recordings were made at 21–23°C using the patch-clamp technique [17] as described in previous reports [16,18]. Junction potentials were measured using a flowing 3 M KCl electrode [16], and the appropriate corrections were applied to our data. The tissue bath was grounded, and potential difference across excised inside-out patches is referenced to the outside, extracellular face, of the membrane. In the cell-attached configuration, potential difference across the patch is equal to the cell membrane potential minus the pipette clamp potential (V_p). Since the membrane potential is unknown, we give V_p values in this recording configuration. Outward current, the flow of positive charge from the inside to the outside of the membrane, is indicated on the figures as an upward deflection from the closed state of the channel. Conductance data were obtained from linear current/voltage (I/V) plots using least-squares regression analysis. Permeability values were determined from I/V plots in inside-out patches using the Goldman equation.

All kinetic analyses were performed off-line, and on patches which contained only one active channel as judged by the absence of multiple current steps. The average record length was 145 ± 30 s, and the number of events 2828 ± 1012. Data were digitised at 10 kHz using a CED 502 interface (Cambridge Electronic Design, Cambridge, UK), and analysed using a Nimbus AX/2 computer (Research Machines, Oxford, UK). Open and closed lifetime distributions were determined using a two-threshold transition algorithm, which employed a 50% threshold crossing parameter to detect events. Single or double exponential probability density functions were fitted to the dwell time histograms using a non-linear least-squares method (software kindly donated by Dr. J. Dempster, University of Strathclyde, U.K). Open state probability (P_0) was calculated as the fraction of total time that channels were open using a minimum of 20 s of data. When multi-channel patches were used for P_0 determinations, we assumed that the total number of channels present was equal to the maximum number of simultaneous current transitions.

Solutions and chemicals

During seal formation, and when recording in the cell-attached mode, the bath contained an extracellular-type, Na^+-rich solution (mM): 138.0 NaCl, 4.5 KCl, 2.0 $CaCl_2$, 1.0 $MgCl_2$, 5.0 glucose, 10.0 Hepes (pH 7.4). In some experiments the chloride in this solution was partially replaced with sulphate or nitrate, and the sodium with *N*-methylglucamine (NMG). Sulphate-replacement (mM): 41.5 NaCl, 47.25 Na_2SO_4, 4.5 KCl, 2.0 $CaCl_2$, 1.0 $MgCl_2$, 70.0 sucrose, 5.0 glucose, 10.0 Hepes (pH 7.4). Nitrate-replacement (mM): 38.0 NaCl, 100.0 $NaNO_3$, 4.5 KCl, 2.0 $CaCl_2$, 1.0 $MgCl_2$, 5.0 glucose, 10.0 Hepes (pH 7.4). *N*-Methylglucamine replacement (mM): 45.0 NaCl, 91.0 NMGCl, 4.5 KCl, 2.0 $CaCl_2$, 1.0 $MgCl_2$, 10.0 Hepes (pH 7.4).

The K^+-rich, intracellular-type, solution contained (mM): 145.0 KCl, 2.0 $CaCl_2$, 1.0 $MgCl_2$, 5.0 glucose, 10.0 Hepes (pH 7.4). In some experiments, the free Ca^{2+}-concentration in this solution was buffered using 2.0 mM EGTA. For ionised calcium levels of 10.0, 1.0, 0.3, 0.1 and 0.01 μM, the total $CaCl_2$ concentrations were 1.997, 1.877, 1.640, 1.205 and 0.263 mM, respectively.

Forskolin (Sigma) was dissolved in ethanol to produce a stock solution of 10 mM, and added to the bath solution to give a final concentration of 1–3 μM. The same volume of ethanol alone had no effect on channel activity. Secretin, dibutyryl cyclic AMP and isobutylmethylxanthine (IBMX), were all made up as concentrated stocks in the appropriate bath solutions. The final bath concentrations were: secretin, 1–10 nM; dibutyryl cyclic AMP, 0.1–1 mM; and IBMX, 0.1–0.5 mM. We have used two different protocols for stimulating the cultured cells. Prolonged stimulation was achieved by exposing the cells to one, or a cocktail, of the stimulants throughout the experimental period, which usually lasted between 0.5 and 6 h. In other experiments, cells were briefly exposed to stimulants while a cell-attached recording was in progress. All other chemicals were purchased from commercial sources and were of the highest purity available.

Statistics

Conductance data were obtained from linear I/V plots by least-squares regression analysis. Significance of difference between means was determined using Student's t-test. The level of significance was set at $P < 0.05$. All values are expressed as mean ± S.E. (number of observations).

Results

Cell-attached patches

Of the 1027 cell-attached patches we obtained on unstimulated duct cells, only one possessed active non-selective cation channels. However, another 53 of these cell-attached patches contained channels which activated following patch excision into solutions containing 2 mM Ca^{2+}. Thus, overall, non-selective cation channels were operational in only 1.9% (1/54) of channel-containing patches on unstimulated cells. In five experiments, exposure of duct cells to stimulants during cell-attached recording did not induce channel activation, despite the fact that all five patches were subsequently shown to contain channels after excision.

Exposing duct cells to stimulants for prolonged periods (0.5–6 h) before giga-seal formation, increased the proportion of cell-attached patches exhibiting active channels to 10/997. Inactive channels were present in another 48 patches so, overall, non-selective cation channels were operational in 17.2% (10/58) of channel-containing patches on stimulated cells. This represents a 9-fold increase compared to unstimulated cells.

Fig. 1A shows cell-attached currents recorded from the apical membrane of a stimulated cell. Four channels are present in this patch, as judged from the maximum number of simultaneous single-channel current steps, and channel activity was voltage-dependent; P_0 increasing from 0.04 to 0.70 as the membrane was depolarized by changing V_p from 30 to −90 mV (Fig. 1A). The single-channel I/V relationship is shown in Fig. 1B. The plot is linear, gives a single-channel conductance of 22 pS, and a reversal potential of −36 mV. In this experiment the pipette contained an Na^+-rich nitrate solution, but similar results were obtained with the standard Na^+-rich and K^+-rich chloride solutions, and with the Na^+-rich sulphate solution (Fig. 1C–E). The mean single-channel conductance was 22 ± 0.8 pS, and the mean reversal potential, which equals the membrane potential if intracellular and pipette cation concentrations are equal, was −42 ± 5 mV ($n = 11$ patches). These results indicate that the channel is cation selec-

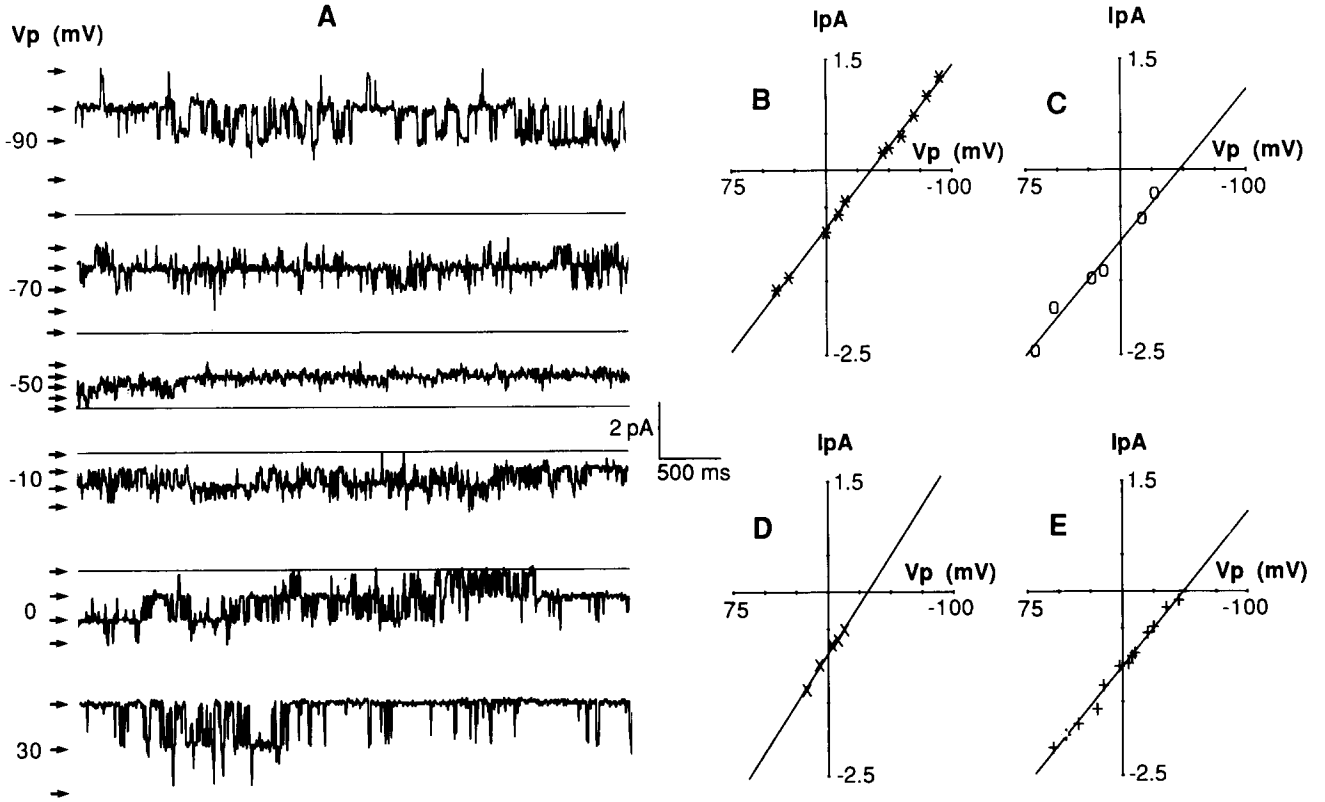

Fig. 1. Single-channel currents in cell-attached patches. (A) Current traces recorded from the apical surface of an intact pancreatic duct pretreated with 1 μM forskolin, 0.1 mM dibutyryl cyclic AMP and 0.1 mM IBMX for 80 min. Low pass filtered at 500 Hz. Solutions: bath, Na^+-rich; pipette, nitrate-replacement. The pipette potential (V_p) is indicated to the left of each trace. Arrows indicate the number of open channels, and the solid line the current level when all channels are closed. There were four active channels in this patch. (B–E) Single-channel I/V plots. (B) Bath, Na^+-rich; pipette, nitrate-replacement. Data taken from records in A. (C) Bath, Na^+-rich; pipette, Na^+-rich. (D) Bath Na^+-rich; pipette, K^+-rich. (E) Bath, Na^+-rich; pipette, sulphate-replacement. Regression lines fitted by least-squares analysis.

tive, and about equally permeable to potassium and sodium. Thus the inward currents recorded at the resting membrane potential ($V_p = 0$ mV trace in Fig. 1A) are carried by sodium ions moving into the cell.

Excised patches

Activity of the non-selective cation channel in excised patches was often quite stable for periods up to 30 min; however, in some experiments, channel activity began to decline within a few minutes of patch excision. There were no obvious differences in the characteristics of channels excised from unstimulated and stimulated cells, and the number (N) of channels per patch (unstimulated, 1.9 ± 0.2, $n = 54$; stimulated, 2.2 ± 0.3, $n = 56$), and the distribution of N were not affected by stimulation (Fig. 2). In experiments on intact ducts (in which the structural polarity of the epithelial cells is retained), the channel was observed in 8.3% (17/204) of patches excised from the basolateral membrane, and in 6.2% (62/999) of patches excised from the apical plasma membrane of the duct cell.

Fig. 3A shows single-channel currents recorded from an inside-out patch bathed in symmetrical Na^+-rich solutions containing 2 mM Ca^{2+}. As in cell-attached recordings, channel activity was voltage-dependent. At depolarizing potentials, the channel was open for most of the time and only very brief closures were observed; however, longer closings became frequent as the membrane was hyperpolarized. While all the channels we examined showed a significant increase in activity with membrane depolarization, absolute P_0 values measured at hyperpolarizing potentials did vary somewhat. The relationship between membrane potential and single channel P_0 is summarised in Fig. 3B. Channel P_0 remained close to the maximum value of 1.0 at positive potentials, but decreased sharply to values below 0.1 when patches were hyperpolarized to potentials lower than -80 mV. Essentially similar results were obtained with both high (mM) and low (10 μM) calcium concentrations on the cytoplasmic face of the membrane (Fig. 3B).

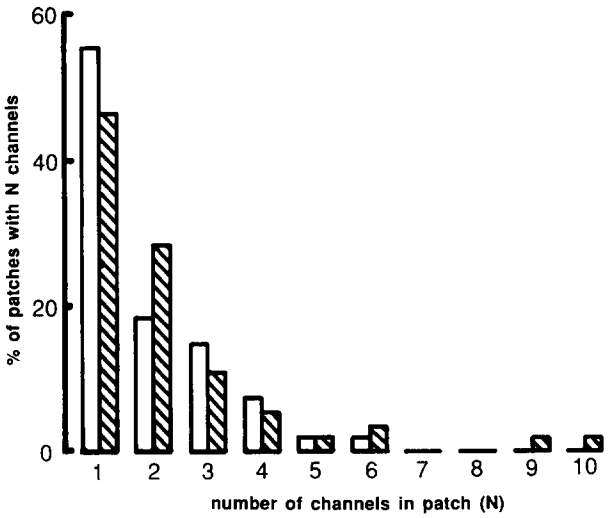

Fig. 2. Number of non-selective cation channels in inside-out patches excised from unstimulated and stimulated duct cells. The number of channels (N) was taken as the maximum number of simultaneous single-channel channel current steps observed during the first 1–2 min of recording immediately after patch excision into a bath solution containing 2 mM Ca^{2+}. Open columns: 54 patches from unstimulated cells. Shaded columns: 56 patches from cells stimulated for 0.5–6 h with a mixture of secretin (1–10 nM), forskolin (1–3 μM), dibutyryl cyclic AMP (0.1–1 mM) and IBMX (0.1–0.5 mM). Sealing rates were 58% for unstimulated cells and 51% for stimulated cells. Patches without channels were not included in the analysis.

The distributions of channel open and closed times in a patch held at -60 mV are shown in Figs. 3D and 3E. Both distributions are best fitted by the sum of two exponentials with time constants of 5.2 and 44.9 ms for the open state, and 2.6 and 37.8 ms for the closed state. In six experiments on different channels the mean values were 2.7 ± 0.5 and 33 ± 6.0 ms for the open state, and 2.2 ± 0.3 and 21 ± 4.0 ms for the closed state. These results suggest that the channel exists in at least two open and two closed states at negative membrane potentials. It proved impossible to obtain an accurate estimate of open and closed times at positive potentials because there were so few closing events; however, visual inspection of the current records suggests that depolarization increases P_0 by eliminating the long-lived closed state, and by greatly increasing open times (Fig. 3A).

When both faces of excised patches were bathed in 150 mM NaCl, the I/V relationship for the non-selective cation channel was linear, reversed at 0 mV, and gave a single-channel conductance of 25.3 ± 0.2 pS ($n = 13$) (Fig. 4A). Similar results were obtained using symmetrical KCl solutions (26.7 ± 0.4 pS, $n = 7$) (Fig. 4B), and when there was an asymmetric distribution of sodium and potassium across the patch (24.2 ± 0.2 pS, $n = 16$) (Fig. 4C). In 11 experiments, we compared the conductance of channels in excised patches with their conductance in cell-attached patches. The mean excised conductance was 25 ± 0.4 pS, which is significantly larger than the value of 22 ± 0.8 pS ($P < 0.003$; paired t-test) obtained in cell-attached patches. This difference in conductance might be explained by a higher concentration of cations in the bath solution as compared to the cell cytoplasm.

Replacing two-thirds of bath sodium with the organic cation N-methylglucamine (keeping chloride concentration constant) caused an inward rectification of the channel currents, and shifted the reversal potential by about 24 mV ($n = 3$) (Fig. 4D). This is slightly less than the value of 26 mV predicted for a cation-selective channel that is impermeable to N-methylglucamine. In contrast, replacing two-thirds of the bath chloride with sulphate, or two-thirds of the pipette chloride with sulphate or nitrate, had no effect on either reversal

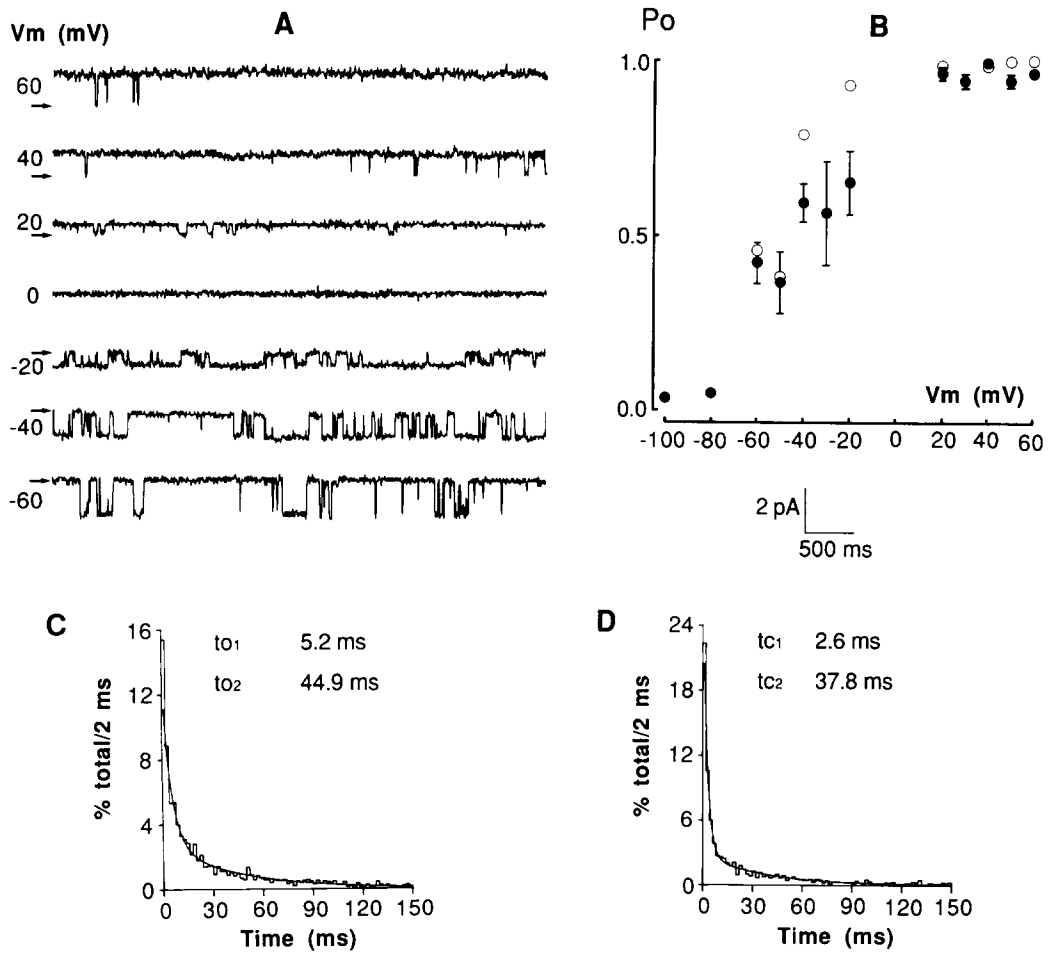

Fig. 3. Effect of membrane potential on channel activity in excised, inside-out patches. (A) Single-channel currents in a patch excised from the basolateral membrane of an intact duct, and exposed to symmetrical Na^+-rich solutions containing 2 mM Ca^{2+}. Low-pass-filtered at 500 Hz. Membrane potential (V_m) is indicated to the left of each trace, and the arrow indicates the closed channel current level. (B) Effect of membrane potential on open-state probability (P_0). Closed symbols (●); data from 10 patches bathed in 2 mM Ca^{2+}. Results are the mean ± S.E. of between 3 and 10 measurements, except for −100 mV which is the mean of two results. Open symbols (○); data from an experiment in which the bath calcium concentration was 10 μM. (C, D) Distribution of channel lifetimes at a membrane potential of −60 mV, calculated from the experiment shown in A. Data filtered at 700 Hz and sampled at 10 kHz. (C) Open time histogram constructed from 1713 events. (D) Closed time histogram constructed from 1747 events. Both distributions were best fitted by the sum of two exponentials which are superimposed on the histograms. Events in the first bin (2 ms) were not included in the fitting procedure.

potential or conductance which was 24.5 ± 0.3 pS (n = 10) under these conditions (Fig. 4E). Increasing the NaCl concentration in the bath solution from 150 to 450 mM (keeping calcium, magnesium and pH constant) caused the reversal potential to shift by −25 mV (Fig. 4F). These results confirm our cell-attached data indicating that the channel is about equally permeable to sodium and potassium but virtually impermeable to anions (Fig. 1), and also show that large organic cations do not permeate the channel. The Na/Cl permeability ratio, calculated from the data in Fig. 4F, is 27/1.

Effect of calcium

Fig. 5A shows that reducing the calcium concentration on the cytoplasmic face of an excised patch from 2 mM to 0.1 μM completely inhibited channel activity. Similar results were obtained in nine other experiments in which the calcium concentration was lowered to between 0.01 to 0.3 μM. At these low calcium levels even strong depolarization did not reactivate the channels, indicating that voltage activation of this non-selective cation channel is calcium-dependent. With 1 μM Ca^{2+}, the results were much more variable and complete inhibition of channel activity was seen in only four out of eight experiments. Of the remaining four patches, channels in two were unaffected by 1 μM Ca^{2+}, while channel activity in the others was inhibited by about 90%. This variability is illustrated in Fig. 5B, which shows current traces from three different patches exposed to 1 μM Ca^{2+}. It is unlikely that this variable response to calcium is caused by exposure of the duct cells to stimulants, because there were no obvious differences in the calcium sensitivity of channels excised from stimulated and unstimulated cells. In three experi-

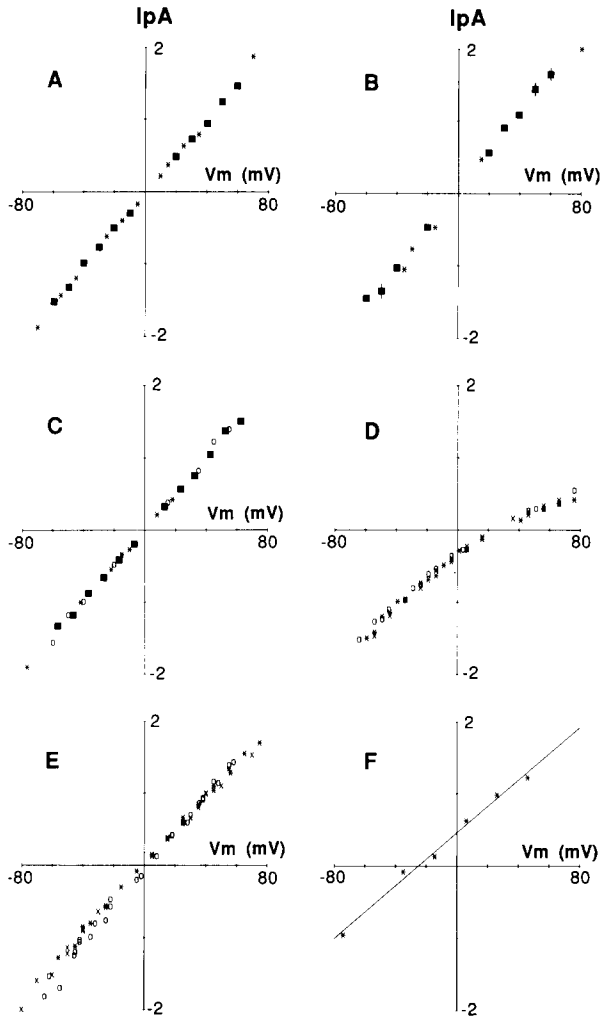

Fig. 4. Effect of anion and cation substitutions on the I/V relationships for channels in excised, inside-out patches. (A) Bath, Na^+-rich; pipette, Na^+-rich (13 patches). (B) Bath, K^+-rich with a final calcium concentration between 1 μM and 2 mM; pipette, K^+-rich (seven patches). (C) Closed symbols: bath, Na^+-rich; pipette, K^+-rich (15 patches). Open symbols: bath, K^+-rich; pipette, Na^+-rich (1 patch). In A, B and C the filled squares represent the mean ± S.E. of 3–14 observations. Error bars are indicated where S.E. exceeds the size of the symbol. (D) Bath, *N*-methylglucamine-replacement; pipette, K^+-rich (three patches indicated by different symbols). (E) Anion substitution. Bath, Na^+-rich; pipette, sulphate-replacement (★———★, three patches). Bath, sulphate-replacement; pipette, K^+-rich (○———○, three patches). Bath, Na^+-rich; pipette, nitrate-replacement (×———×, four patches). (F) Bath, 450 mM NaCl; pipette, Na^+-rich (1 patch). The line in F was fitted by least-squares regression analysis.

ments, channel activity was unaffected by reducing the calcium concentration on the cytoplasmic face of the membrane from 2 mM to 10 μM. Low calcium solutions did not affect channel conductance.

Effect of magnesium

Fig. 6 shows that reducing the magnesium concentration on the cytoplasmic face of an excised patch from the standard 1 mM to nominally zero (maintaining calcium constant at 2 mM) increased P_0 by 36% from 0.661 to 0.900. On replacing magnesium, channel P_0 returned to 0.667, showing that the effect of magnesium withdrawal can be fully reversed (Fig. 6). This activating effect of magnesium removal was only observed at hyperpolarizing potentials; when the same patch was voltage clamped at 60 mV, and then exposed to a magnesium-free solution, channel P_0 was unaffected. This suggests that either low magnesium alters the voltage-dependence of channel gating, or that the binding of magnesium is voltage-dependent. Similar results were obtained in two other experiments.

Effect of pH

Fig. 7A shows that an increase in cytoplasmic surface pH, from the standard value of 7.4 to 7.9, markedly reduced channel activity. On the other hand, we found that decreasing cytoplasmic pH from 7.4 to 6.9. had no effect on the channel. The inhibitory effect of alkalinisation was not dependent on membrane potential, was fully reversible, and was observed in seven out of eight experiments on different patches. In contrast, no effects on channel activity were observed in four experiments

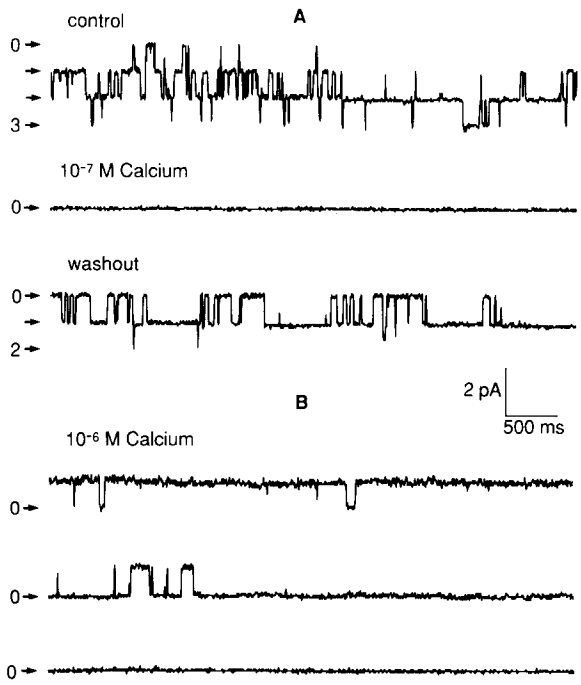

Fig. 5. Effect of cytoplasmic calcium concentration on channel activity in excised, inside-out patches. (A) Single-channel currents recorded from a patch exposed to 2 mM Ca^{2+} (top trace), 0.1 μM Ca^{2+} (middle trace) and then 2 mM Ca^{2+} again (bottom trace). Low-pass-filtered at 500 Hz. Membrane potential was −40 mV. Number of open channels is indicated to the left of each trace. The decline in channel number seen during the experiment is unlikely to have been caused by exposure to low calcium, since this phenomenon was also observed in patches bathed only in 2 mM Ca^{2+}. (B) Single-channel currents recorded from three patches bathed in K^+-rich solutions containing 1 μM Ca^{2+}. Membrane potential was 40 mV. Low-pass-filtered at 500 Hz.

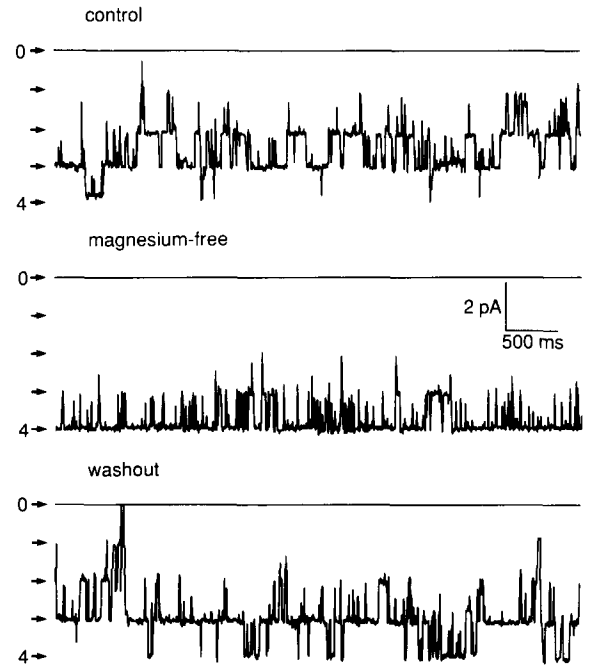

Fig. 6. Effect of cytoplasmic magnesium concentration on channel activity in excised, inside-out patches. Solutions: bath, Na^+-rich; pipette, Na^+-rich. Channel currents recorded from a patch exposed to 1 mM Mg^{2+} (top trace), a nominally Mg^{2+}-free solution (middle trace), and 1 mM Mg^{2+} again (bottom trace). Low-pass-filtered at 500 Hz. Membrane potential was −60 mV. Number of open channels is indicated to the left of each trace.

in which the orientation of the pH gradient across the membrane was reversed by increasing pipette solution pH to 7.9. Furthermore, under these conditions, channel activity was still inhibited by alkalinisation on the cytoplasmic face of the membrane (Fig. 7B), demonstrating that cytoplasmic pH, and not a transmembrane pH gradient, modulates the channel.

Effect of ATP and ADP

Fig. 8A and B show that ATP and ADP (1 mM) inhibited channel activity when applied to the cytoplasmic surface of excised patches. This inhibition was observed in four separate experiments with each nucleotide, and was fully reversible (Fig. 8A and B). The reduction in channel activity caused by ATP was dose-dependent and, at ATP concentrations below 1 mM, also voltage-dependent (Fig. 8C). ATP was a much less effective inhibitor of channel activity at depolarising potentials, the concentration required to produce a 50% reduction in P_0 being 395 ± 57 μM at potentials between 40 and 60 mV, and 174 ± 43 μM at potentials between −40 and −60 mV (Fig. 8C). This inhibitory effect of ATP did not require the presence of magnesium, so it probably results from a direct interaction of the nucleotide with the channel, and not from channel phosphorylation catalysed by a membrane-bound kinase.

Effect of cation channel blockers

A variety of cation channel blockers were also tested for their ability to interact with the non-selective channel. Barium (1 mM, two experiments), TEA (10 mM, four experiments), and decamethonium (0.5 mM, one experiment) had no effect on either channel activity or conductance when applied to the cytoplasmic surface of excised patches. In contrast, 0.5 mM quinine produced a marked change in channel activity, characterised by appearance of many brief closing events (channel flickering) without alteration in single-channel current amplitude. The degree of quinine-induced flickering was dependent on membrane potential, and increased as the patch was depolarized, i.e., as the driving force for quinine entry into the channel was increased. Channel block was fully reversed after washout of quinine from the bath solution (Fig. 9).

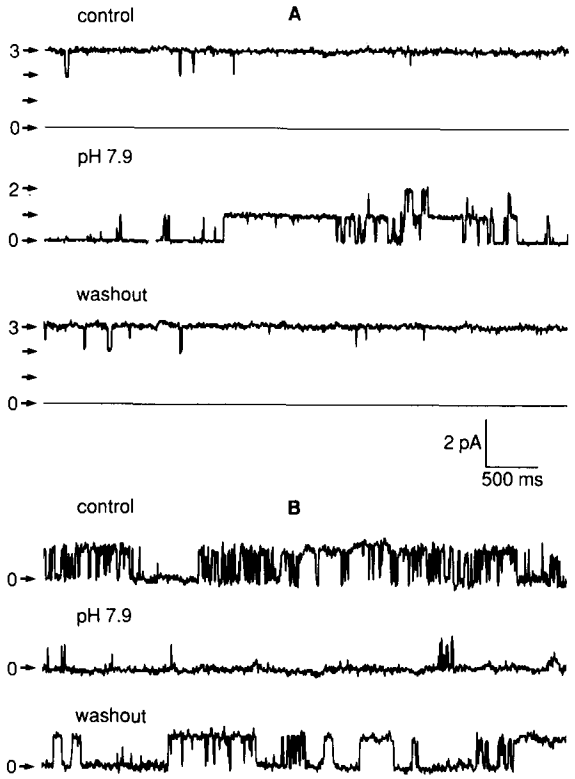

Fig. 7. Effect of cytoplasmic pH on channel activity in excised, inside-out patches. (A) Channel currents recorded with bath and pipette solutions buffered at pH 7.4 (top trace); after changing the bath solution to pH 7.9 (middle trace), and after switching back to pH 7.4 (bottom trace). All solutions were Na^+-rich and membrane potential was 45 mV. Low-pass-filtered at 500 Hz. Number of open channels is indicated to the left of each trace. (B) Current traces recorded with the bath solution buffered at pH 7.4 and the pipette solution buffered at pH 7.9 (top trace); after changing the bath solution to pH 7.9 (middle trace), and after switching back to pH 7.4 (bottom trace). Low-pass-filtered at 500 Hz. All solutions were Na^+-rich and membrane potential was 60 mV. Arrows indicate the closed channel current level.

Discussion

Using the patch clamp technique, we have identified a non-selective cation channel located on the basolateral and apical membranes of rat pancreatic duct cells. The channel has a conductance of about 25 pS, is equally permeable to sodium and potassium, has a low permeability to anions, and is activated by membrane depolarization provided the cytoplasmic calcium concentration is $\geq 1\ \mu M$. The K^+ channel blockers, barium and TEA, had no effect on channel activity, but quinine caused a flickering block which was more pronounced at depolarizing potentials. Non-selective cation channels with similar properties have been identified in nerve [2,3,11], muscle [19] and endocrine cells [20–22], and also in a number of different epithelial cell types [5–10,23–27].

As in cardiac muscle [19], neuroblastoma cells [2], thyroid cells [23] and mast cells [22], we found that calcium concentrations of around 1 μM were required to activate the duct cell channel in excised patches, although the level of channel activity varied consider-

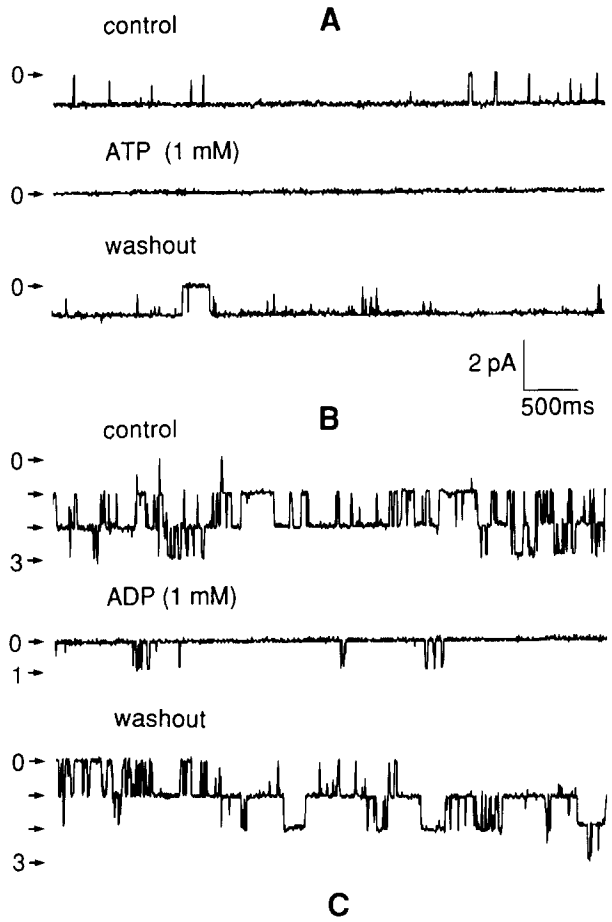

Fig. 8. Effect of cytoplasmic ATP and ADP on channel activity in excised, inside-out patches. (A) Channel currents recorded without ATP (top trace), with 1 mM-MgATP (pH 7.4 and 2 mM Ca^{2+}) (middle trace), and after washout of ATP (bottom trace). Low-pass-filtered at 500 Hz. All solutions were Na^+-rich and membrane potential was −50 mV. Arrow indicates the closed channel current level. (B) Channel currents recorded without ADP (top trace), with 1 mM MgADP (pH 7.4 and 2 mM Ca^{2+}) (middle trace), and after washout of ADP (bottom trace). All solutions were Na^+-rich and membrane potential was −50 mV. Low-pass-filtered at 500 Hz. Number of open channels is indicated to the left of each trace. (C) Dose-response curves for the effect of ATP on channel activity at positive (●) and negative (○) membrane potentials. P_0 is expressed as a percentage of the control value measured in the absence of ATP. Data from 14 patches. Each point is the mean ± S.E. of 3–5 measurements on separate patches. Positive potentials were between 40 and 60 mV and negative potentials between −40 and −60 mV.

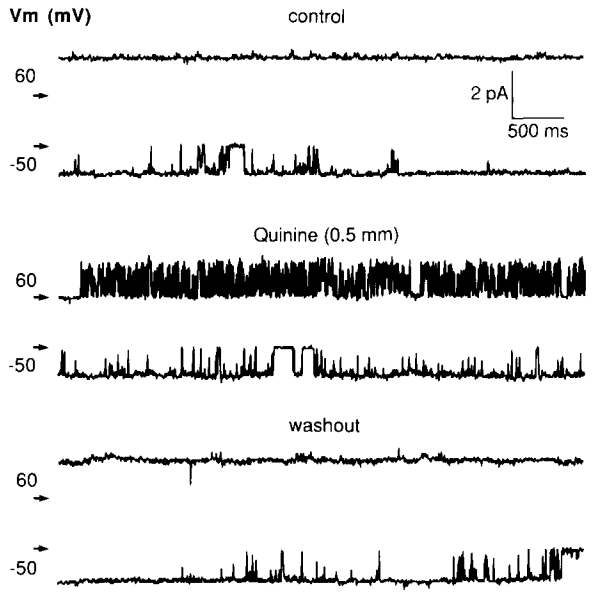

Fig. 9. Effect of cytoplasmic quinine on channel activity in excised, inside-out patches. Channel currents recorded without quinine (top two traces), with 0.5 mM quinine (middle two traces), and after washout of quinine (bottom two traces). All solutions were Na^+-rich and the membrane potential (V_m) is indicated to the left of each trace. Low pass filtered at 500 Hz. Arrows indicate the closed channel current level.

ably in different experiments. This contrasts with channels in Schwann cells [3], lacrimal acinar cells [8], the islet cell line CRI-G1 [21], cultured proximal tubule cells [26], and human neutrophils [4] which are all much less sensitive to calcium, requiring 10 to 100 μM Ca^{2+} for channel activation. Such a wide variation in calcium responsiveness may indicate that a factor which confers calcium sensitivity is lost following patch excision. This has previously been shown for pancreatic acinar cell channels which can be activated by 0.1 μM Ca^{2+} immediately after excision, but whose calcium sensitivity declines subsequently [7]. Provided calcium (≥ 1 μM) was present on the cytoplasmic face of the membrane, opening of the duct cell channel was also increased by depolarization such that P_0 values were close to 1.0 at positive membrane potentials. The P_0 of most non-selective cation channels is not affected by voltage; however, channels in Schwann cells [3], CRI-G1 cells [21] and neutrophils [4] are activated by depolarization, although in Schwann cells voltage-activation was found to be more pronounced at low calcium concentrations, an effect we have not observed.

Analysis of channel lifetime distributions performed on inside-out patches at physiological potentials indicated that the channel must exist in at least two open and two closed states. A similar result was reported for non-selective cat ion channels in Schwann cells [3] and CRI-G1 cells [21]. Depolarization appears to activate the channel by increasing the duration of open times, and also by removing the long-lived closed state. We also show that the voltage-dependence of channel opening can be affected by magnesium, in as much as the long closed periods disappear in Mg^{2+}-free solutions, at least over the potential range ± 90 mV. This might be caused by low magnesium shifting the P_0/voltage relationship towards negative potentials; a possibility we were unable to check because patches held at high negative potentials (more than -100 mV) were very unstable. Effects of magnesium on the gating of non-selective cation channels have not previously been reported; however, magnesium withdrawal does increase the activity of ATP-sensitive K^+ channels in the insulin-secreting RINm5F cell [28], and in ventricular myocytes [29]. In contrast, Ca^{2+}-activated maxi-K^+ channels in skeletal muscle t-tubules [30] and salivary acinar cells [31] are inhibited by magnesium withdrawal, possibly due to a reduction in their calcium sensitivity.

We also show that an increase in cytoplasmic pH from 7.4 to 7.9 markedly reduced channel activity but, surprisingly, that a decrease in pH from 7.4 to 6.9 had no effect. An action of pH on non-selective cation channels has not, to our knowledge, previously been reported; however, it is well known that Ca^{2+}-sensitive K^+ channels are inhibited by cytoplasmic acidification and activated by cytoplasmic alkalinisation, i.e., their response to pH is opposite to that of the non-selective channel [32]. These effects of pH on K^+ channels are probably explained by competition between protons and calcium for the calcium binding site on the channel, which causes a shift in the P_0/voltage relationship [32]. A similar mechanism cannot explain the action of pH on the non-selective channel because alkalinisation decreased, rather than increased, channel activity. Furthermore, the inhibitory effect of alkalinisation was not voltage-dependent, suggesting that the P_0/voltage relationship was unaltered.

Adenine nucleotides block non-selective cation channels in CRI-G1 cells [20,21] and pancreatic acinar cells [25], and here we show that they are also effective inhibitors of the duct cell channel. Both ATP and ADP caused an essentially complete inhibition of channel activity at a concentration of 1 mM. Since ATP was effective in the absence of magnesium, it is unlikely that phosphorylation is involved in channel inhibition. This result also indicates that both the free acid and the divalent cation bound forms of ATP are effective in closing the channel. The blocking effect of ATP was dose-dependent and, at concentrations between 0.1 and 0.5 mM, also voltage-dependent. The ATP-concentration producing a 50% reduction in channel P_0 was 174 μM at negative potentials, and 395 μM at positive membrane potentials. These values are 20- to 50-fold higher than those reported for the voltage-independent ATP block of non-selective cation channels in CRI-G1 cells [21]. Our finding that the duct cell channel is blocked by 1 mM ATP, and also requires around 1 μM Ca^{2+} for activity, may explain why it was so rarely observed in cell-attached patches.

Non-selective cation channels are thought to play an important role in NaCl and fluid secretion from pancreatic [5–7,25] and lacrimal acinar cells [8] by providing a pathway for sodium and possibly calcium uptake into the cell. In these cells, the channel is activated by acute exposure to secretory agonists via an increase in intracellular calcium concentration [6,8]. Pancreatic duct cells secrete the bicarbonate ions found in pancreatic juice [12]; most likely by an electrogenic mechanism involving parallel operation of Cl/HCO_3 exchangers and a regulated chloride channel [16,18,33,34]. We never observed channel activation following acute exposure of duct cells to stimulants, which suggests that the channel is not involved directly in bicarbonate transport. However, prolonged stimulation did cause a 9-fold increase in the proportion of cell-attached patches which contained active channels. The cellular mechanism responsible for this effect, and its physiological significance, are unclear since opening of the channel would cause an inwardly-directed sodium current which would depolarise the cell, and hence reduce the driving force for bicarbonate secretion. However, it is possible that the sodium influx is part of a volume regulatory response which offsets the stimulation-induced shrinkage that

occurs in exocrine gland cells [35]. Despite this uncertainty as to its precise physiological role, the fact that the non-selective cation channel is regulated by a number of physiologically important parameters (calcium, magnesium, voltage, pH and adenine nucleotides) does suggest that it plays some part in duct cell function.

Acknowledgements

We thank Dr. J. Dempster, University of Strathclyde, U.K. for computer programs, Dr. S. Arkle for help with preliminary experiments, and Mr. N. Hampton for assistance with data analysis. Supported by the Medical Research Council (U.K.), and a small grants research award from the University of Newcastle upon Tyne.

References

1 Partridge, L.D. and Swandulla, D. (1988) Trends Neurol. Sci. 11, 69–72.
2 Yellen, G. (1982) Nature 296, 357–359.
3 Bevan, S., Gray, P.T.A. and Ritchie, J.M. (1984) Proc. R. Soc. London B 222, 349–355.
4 Von Tscharner, V., Prod'hom, B., Baggiolini, M. and Reuter, H. (1986) Nature 324, 369–372.
5 Maruyama, Y. and Petersen, O.H. (1982) Nature 299, 159–161.
6 Maruyama, Y. and Petersen, O.H. (1982) Nature 300, 61–63.
7 Maruyama, Y. and Petersen, O.H. (1984) J. Membr. Biol. 81, 83–87.
8 Marty, A., Tan, Y.P. and Trautmann, A. (1984) J. Physiol. 357, 293–325.
9 Light, D.B., McCann, F.V., Keller, T.M. and Stanton, B.A. (1988) Am. J. Physiol. 255, F278–F286.
10 Light, D.B., Schwiebert, E.M., Karlson, K.H. and Stanton, B.A. (1989) Science 243, 383–385.
11 Partridge, L.D. and Swandulla, D. (1987) Pflügers Arch. 410, 627–631.
12 Case, R.M. and Argent, B.E. (1989) in Handbook of Physiology: The Gastrointestinal System (Schultz, S.G., Forte, J.G. and Rauner, B.B., eds.), Vol. III (Section 6), pp. 383–417, Oxford University Press, New York.
13 Argent, B.E., Arkle, S., Gray, M.A. and Greenwell, J.R. (1987) J. Physiol. 386, 82P.
14 Arkle, S., Lee, C.M., Cullen, M.J. and Argent, B.E. (1986) Q. J. Exp. Physiol. 71, 249–265.
15 Argent, B.E., Arkle, S., Cullen, M.J. and Green, R. (1986) Q. J. Exp. Physiol. 71, 633–648.
16 Gray, M.A., Greenwell, J.R. and Argent, B.E. (1988) J. Membr. Biol. 105, 131–142.
17 Hamill, O.P., Marty, A., Neher, E., Sakmann, B. and Sigworth, F.J. (1981) Pflügers Arch. 391, 85–100.
18 Gray, M.A., Harris, A., Coleman, L., Greenwell, J.R. and Argent, B.E. (1989) Am. J. Physiol. 257, C240–251.
19 Colquhoun, D., Neher, E., Reuter, H. and Stevens, C.F. (1981) Nature 294, 752–754.
20 Sturgess, N.C., Hales, C.N. and Ashford, M.L.J. (1986) FEBS Lett. 208, 397–400.
21 Sturgess, N.C., Hales, C.N. and Ashford, M.L.J. (1987) Pflügers Arch. 409, 607–615.
22 Lindau, M. and Fernandez, J.M. (1986) J. Gen. Physiol. 88, 349–368.
23 Maruyama, Y., Moore, D. and Petersen, O.H. (1985) Biochim. Biophys. Acta 821, 229–232.
24 Teulon, J., Paulais, M. and Bouthier, M. (1987) Biochim. Biophys. Acta 905, 125–132.
25 Suzuki, K. and Petersen, O.H. (1988) Am. J. Physiol. 255, G275–G285.
26 Merot, J., Bidet, M., Gachot, B., Le Maout, S., Tauc, M., Poujeol, P., Othmani, L. and Gastineau, M. (1988) Pflügers Arch. 413, 51–61.
27 Gögelein, H. and Pfannmüller, B. (1989) Pflügers Arch. 413, 287–298.
28 Findlay, I. (1987) J. Physiol. 391, 611–629.
29 Findlay, I. (1987) Pflügers Arch. 410, 313–320.
30 Golowasch, J., Kirkwood, A. and Miller, C. (1986) J. Exp. Biol. 124, 5–13.
31 Squire, L.G. and Petersen, O.H. (1987) Biochim. Biophys. Acta 899, 171–175.
32 Cook, D.L., Ikeuchi, M. and Fujimoto, W.Y. (1984) Nature 311, 269–271.
33 Novak, I. and Greger, R. (1988) Pflügers Arch. 411, 58–68.
34 Novak, I. and Greger, R. (1988) Pflügers Arch. 411, 546–553.
35 Burgen, A.S.V. (1967) in Handbook of Physiology: Alimentary Canal (Code, C.F., ed.), Vol. II (Section 6), pp. 562–575, American Physiological Society, Washington.